Single particle ICP-MS combined with a data evaluation tool as a routine technique for the analysis of nanoparticles in complex matrices

Journal:	*Journal of Analytical Atomic Spectrometry*
Manuscript ID:	JA-ART-10-2014-000357.R2
Article Type:	Paper
Date Submitted by the Author:	04-Jan-2015

Complete List of Authors:	Peters, R J B; RIKILT - Wageningen UR, Herrera-Rivera, Zahira; RIKILT - Wageningen UR, Undas, Anna; RIKILT - Wageningen UR, van der Lee, Martijn; RIKILT - Wageningen UR, Marvin, H.J.P.; RIKILT - Wageningen UR, Bouwmeester, Hans; RIKILT Wageningen UR, ; RIKILT - Wageningen UR, Weigel, Stefan; RIKILT Wageningen UR, ; RIKILT - Wageningen UR,

Single particle ICP-MS combined with a data evaluation tool as a routine technique for the analysis of nanoparticles in complex matrices

Ruud Peters, Zahira Herrera-Rivera, Anna Undas, Martijn van der Lee, Hans Marvin, Hans Bouwmeester, Stefan Weigel

RIKILT – Wageningen UR, PO Box 230, 6700 AE Wageningen, the Netherlands

Abstract

Detection and characterization of nanoparticles (NPs) in complex media as consumer products, food and toxicological test media is an essential part of understanding the potential benefits and risks of the application of nanoparticles. Single particle ICP-MS (spICP-MS) was studied as a screening tool for the detection and characterization of nanoparticles in complex matrices such as food and biological tissues. A data evaluation tool was created for the calculation of particle size, concentration and size distribution from the raw data. spICP-MS measurements were carried out on a standard quadrupole instrument as well as on a sector-field instrument. Performance characteristics were determined for four types of NPs. For the quadrupole instrument the size detection limits were 20 nm (Au and Ag), 50 (TiO_2) and 200 nm (SiO_2). For the sector-field instrument size detection limits are lower, 10 nm (Au). Concentration detection limits ranged from 1 ng/L for 60 nm Au NPs to 0.1 µg/L for 500 nm SiO_2 particles. The dynamic range of spICP-MS is limited to two orders of magnitude and as a consequence sample dilution is often required. The precision of the method was found to be <5% and <10% for the determination of particle size and concentration, respectively while the accuracy for particle size (Au NP only) was <10%. The robustness against potential sample matrix components was investigated. The applicability to routine samples was demonstrated by four examples (food, waste water, culture media and biological tissues).

The presented combination of spICP-MS measurements with a powerful data evaluation tool enables the use of this technique as a fast, cost efficient and easy to use screening tool for metal and metal oxide NPs that can be widely implemented in the statutory monitoring of food and consumer products for the presence of NPs, as well as in the analytical evaluation of toxicological studies.

1. Introduction

The potential benefits of the application of nanotechnology are widely recognized. Products based on nanotechnology or containing engineered nanoparticles (ENPs) are already manufactured in the field of electronics, construction, medicine, textiles, cosmetics, food and other consumer products[1]. Applications in the food sector include the use of nano-formulated ingredients and additives. A number of conventional approved food additives have a size distribution that involves a fraction in the size range below 100 nm. Examples with high usage volumes are fumed silica (approved in the European Union as E551) and titanium dioxide (E171). Furthermore, engineered nanomaterials may enter food by migration of ENP from food contact materials (e.g. packaging) or from environmental contamination. Clearly, a variety of nanoparticles (NPs, e.g. silver, silica, titanium-, zinc- and iron oxides) are known or claimed to be used and therefore it is likely that consumers will be directly or indirectly exposed. However, due to the relative novelty of ENPs, the assessment of the risks for the environment and human health has only recently started. Detection and characterization of NPs in food and in samples from biological and toxicological tests is an essential part of understanding the potential benefits as well as the potential risks of the application of ENPs[2,3,4].

In contrast to methods for the characterisation of pure nanomaterials analytical methods for the determination of ENP in complex matrices such as food have to cope with a number of additional requirements. Target particles have to be removed from the matrix, separated from interfering matrix components and naturally occurring particles and enriched in the extract to meet the quantification limits of the detection instruments. Routine methods for a statutory monitoring of the presence of ENP in food also have to be cost-efficient. A recommendation for a definition of a nanomaterial published by the European Commission states that “in a nanomaterial more than 50% of the number of particles in an unbound state or as an aggregate or as an agglomerate, are in the size range of 1 to 100 nm”[5]. This inherently requires methods that produce reliable particle number size distributions.

Currently, separation techniques as hydrodynamic chromatography (HDC) and field flow fractionation (FFF) are used to determine NPs in combination with detectors such as multiple angle light scattering (MALS) and inductive coupled mass spectrometry (ICP-MS) in order to achieve a reliable and quantitative determination of ENP [6,7,8,9,10,11] . For these methods, sample preparation is often required prior to instrumental analysis with the aim of removing interfering matrix components and to

meet the required detection limits. Few methods are available for the respective sample preparation and the methods that are available are often difficult and time consuming.

The only direct way to determine true particle number size distributions is to use a single particle counting method. Several methods are available: electron microscopy is most widely used to generate particle number based size distributions of a wide range of particles, nanoparticle tracking analysis (NTA) is used to determine number based size distributions in liquids while differential mobility analyzers (DMA) are used in aerosol analysis[12,13]. spICP-MS can also generate a particle number based size distribution and since ICP-MS is widely available in many laboratories this is an interesting technique to characterize NPs.

The concept of utilizing ICP-MS for single particle analysis and colloid suspensions was first published by McCarthy and Degueldre[14] and tested for a series of particles in aqueous suspensions. More recently, spICP-MS has been described as a tool for the determination of NPs[15] and various applications have been described: Au in bio-analytical samples[16,17], Pb in airborne particles[18], dissolved and particulate Ag[19,20,21]. Recently, fully validated analytical methods using spICP-MS have been published[22], and the suitability of the method has been tested in interlaboratory exercises[23,24]. In spICP-MS, metal or metal oxide based NPs in a sample are introduced into the ICP-MS producing a plume of metal ions in the plasma torch. This plume is detected as a signal pulse in the mass spectrometer and allows the determination of the NP concentration in the sample as well as the mass of the metal in the individually detected NPs. Based on the particle mass, composition, density and an assumed particle shape, the particle size can be estimated. Adequate time resolution and a low particle concentration are required to ensure that each signal pulse originates from one particle only, hence the name “single particle” ICP-MS. As a consequence, samples generally have to be diluted to reach a particle number concentration that is low enough to ensure that the probability of detecting two or more particles simultaneously can be neglected. Since sample dilution also results in a dilution of the matrix, matrix interferences are minimized which is a fast and easy alternative for the often more complex sample preparation techniques and therefore is spICP-MS an interesting technique for screening of metal- and metal oxide based NPs in complex matrices[25].

This paper describes the suitability of spICP-MS for routine analysis, including adequate and simple sample preparation methods, performance characteristics, matrix effects, and most importantly, a spreadsheet tailored for the processing of spICP-MS data. In principle, data from each type and brand of ICP-MS can be

imported in the spreadsheet that allows for calculation of particle size, particle size distribution and the mass- and number-based particle concentration. Practical applications for the determination of NPs in food, waste water and biological samples originating from *in-vitro* and *in-vivo* experiments are shown.

2. Experimental section

2.1 Materials and chemicals

spICP-MS was tested and validated using the NIST reference materials RM8011, -8012 and -8013, citrate stabilized Au NPs with nominal diameters of 10 nm, 30 nm and 60 nm in aqueous suspension at a mass concentration of 0.005%. Ag NPs with particle diameters of 20, 30, 60 and 110 nm were acquired from NanoComposix (San Diego, USA), and consisted of an aqueous suspension in 2 mM sodium phosphate buffer with a mass concentration of 0.1%. For an *in-vivo* experiment Ag NPs with a diameter <20 nm (NM-300K) were obtained from the JRC (Italy). TiO_2 NPs of 25, 40 and 180 nm were purchased from NanoComposix (San Diego, USA) and consisted of a fine white powder. Another powdered TiO_2 nanomaterial with diameter <100 nm was purchased from Sigma Aldrich (Wisconsin, USA). Aqueous suspensions of these TiO_2 NPs were prepared by sonication of a suspension of 8 mg powder in 2 mL water three times 20 minutes prior to further dilution. Suspensions of SiO_2 NPs with diameters of 100 nm to 10 µm were a kind gift of F. von der Kammer, University of Vienna, Austria. Diluted suspensions of all NPs were prepared in MilliQ water after sonication of the NP stock suspensions for 15 minutes.

A solution of proteinase K, 822 u/mL, was obtained from Fermentas (Fisher Scientific, Landsmeer, The Netherlands). Triton X-100, SDS, NaCl, EDTA, methanol and calcium acetate monohydrate ($Ca(CH_3CO_2)2{\cdot}H_2O$) were obtained from Sigma-Aldrich (St. Louis, MO,USA), Tris-buffer (hydroxymethyl aminomethane, H2NC(CH2OH)3) was obtained from Merck (Darmstadt, Germany). The digestion buffer was prepared by dissolving 600 mg of Tris-buffer and 90 mg of calcium acetate monohydrate in 200 mL MilliQ water. 5 mL of Triton X-100 was added to the solution and mixed with a magnetic stirrer until completely dissolved. This solution was further diluted with MilliQ water until a final volume of 500 mL. A MilliQ-Plus ultrapure water system from Millipore (Amsterdam, The Netherlands) was used to

obtain high purity water used during sample preparation and dilution of standards and sample suspensions.

2.2 Instrumentation

ICP-MS. Two different types of ICP-MS systems were used in this study, a quadrupole based Thermo Scientific X-series 2, and a Thermo Finnigan Element 2, a sector field based ICP-MS. Both ICP-MS systems were equipped with a standard nebulizer and a quartz impact bead spray chamber. The Thermo Scientific X-series 2 was operated at a forward power of 1400 W and the gas flows were at the following settings; plasma, 13 L/min; nebulizer, 1.1 L/min; auxiliary, 0.7 L/min. The sample flow rate to the nebulizer was set at 1.5 mL/min using the integrated peristaltic pump. Data acquisition was done using the Thermo PlasmaLab software in the time resolved analysis (TRA) mode. The dwell time was set at 3 ms with typical acquisition times of 60 s per measurement. Isotopes monitored were the following: gold (m/z 197), silver (m/z 107), titanium (m/z 48) and silicon (m/z 28).
The Thermo Element 2 was operated at a forward power of 1000 W and the gas flows were at the following settings; plasma, 15 L/min; nebulizer, 1.1 L/min; auxiliary, 1.2 L/min. The sample flow rate to the nebulizer was set at 1.0 mL/min using the integrated peristaltic pump. Data acquisition was done using the Thermo Element 2 software in the time resolved analysis (TRA) mode. For the measurement of gold (m/z/ 197) and silver (m/z 109) the spectrometer was used in low resolution mode while titanium (m/z 47.78) and silicon (m/z 28.09) were measured in medium resolution mode. In both modes the instrument measures not one mass but a range of slightly differing masses closely around the monitored isotope and two different masses (typically 0.01 amu apart) have to monitored as a minimum. Measuring a single mass as with quadrupole instruments is not possible. In this study typically 3 masses are measured, the monitored isotope and one mass left and one mass right from the monitored isotope. The dwell time was set at 2 ms which means that the instrument measures 2 ms for each mass, i.e. 3x2 ms for each data point.
The nebulization efficiency was determined by the analyses of NIST material RM8013 at a concentration of 50 ng/L under the same instrumental conditions as the samples, monitoring m/z 197 for gold. The nebulization efficiency was calculated from the observed number of particles in the time scan and the particle flux into the ICP-MS system. This, and other methods are described by Pace et al.[15]. Mass calibration curves were determined by the measurement of ionic standard solutions

of the respective elements. Data were exported as csv files to be processed by the developed data evaluation tool in Microsoft Excel.

Data evaluation tool. Data evaluation is carried out using a dedicated spreadsheet, the Single Particle Calculation spreadsheet that was developed in house. The SPC spreadsheet consists of two worksheets, a calibration worksheet and a sample calculation worksheet. For each series of measurement the data of the particle standard (RM8013) in that sample series is entered in this worksheet to calculate the nebulization efficiency η_n. The response factor of an ionic analyte standard, RF_{ION}, of the element to be measured is also entered in this worksheet. The required data are automatically copied to the sample worksheets for calculation of particle sizes and concentrations in sample extracts. Further description of the spreadsheet and it's use can be found in the Result section. The SPC spreadsheet and a procedure for performing spICP-MS measurements including the SPC spreadsheet can be downloaded from the RIKILT website: http://www.wageningenur.nl/en/Expertise-Services/Research-Institutes/rikilt/Software-and-downloads.htm.

2.3 Samples and sample processing

Generally, aqueous samples containing NPs were sonicated for 10 min with a Misonix XL-2000 sonicator equipped with a CML-4 needle probe at 22.5 KHz and 4 W power.

Food: Samples of chicken meat fortified with silver NP were obtained from the EC Joint Research Centre – Institute of Reference Materials and Measurements. These samples were prepared as reference materials in the framework of the NanoLyse project and were doped with 0.1 and 0.5 g/kg, respectively, of 60 nm Ag NP. Details of the preparation are reported elsewhere [26]. Enzymatic digestion of the sample was carried out in two steps. First, 4 mL of the digestion buffer (10 mM Tris buffer, 1% Triton x-100 and 1 mM calcium acetate at pH 9.5) was added to the sample in a 10 mL PE tube, the sample was vigorously vortexed for 1 min and tip sonicated at 4 W power for 5 min. During sonication the sample tube was placed in an ice bath to avoid an increase of the sample temperature. Second, 25 µL of a proteinase K solution was added and the tube was incubated for 3 hrs at 35°C. After cooling to room temperature the digest was diluted with MilliQ water and measured using spICP-MS.

Waste water: Waste water samples containing Ag NPs were supplied by Alterra Wageningen UR. The sample was sonicated for 10 minutes and diluted in MilliQ water.

Culture media: Samples of the apical and basolateral pole of a monolayer of intestine cells after 24 hours exposure to TiO_2 NPs in a translocation experiment were used. The samples were sonicated for 10 min prior to dilution in MilliQ water and analysis with spICP-MS.

Biological tissues: Rat liver samples of an oral exposure study with Ag NPs were used. A 200 mg subsample of the liver was collected, cut into small pieces and mixed with 2 mL of the digestion buffer (10 mM Tris buffer, 1% Triton x-100 and 1 mM calcium acetate at pH 9.5). 25 µL of proteinase K solution was added and the tube was incubated for 16 hrs at 55°C for enzymatic sample digestion. After cooling to room temperature the digest was diluted with MilliQ water and measured using spICP-MS.

2.4 Determination of performance characteristics

The size detection limits (LOD_{SIZE}) in spICP-MS were estimated by plotting the signal intensity I_p as a function of the diameter to the 3th power (d^3) and verified by the measurement of suspensions of particles of the respective diameters, thus accounting for background level effects. The concentration detection limit (LOD_{CONC}) is given by the number of particles in a sample that can significantly be distinguished from the number of particles in a blank sample. The LOD_{CONC} was therefore determined by the measurement of blank samples (before and between actual sample series) as number of particles in blank + 3 x SD (and subsequently transformed to particle and mass concentrations). The dynamic range was determined by measuring suspensions of one particle size at increasing particle concentrations and expressed as the linear range (correlation coefficient) of the resulting calibration curves. Similarly, the upper particle size limit was determined by the measurement of suspensions of particles of increasing size. The precision was determined by replicate analysis (n=6) of standard dispersions in water. Accuracy was determined by replicate analysis (n=6) of NIST reference materials RM8011, -8012 and -8013. Robustness against different components that were expected in the target matrices was evaluated by the determination of the particle concentration and particle size of 60 nm Au, 60 nm Ag and <100 nm TiO_2 NPs in water containing the following matrix components at three concentration levels: sodium dodecyl sulphate

(SDS: 1 to 10 mM), methanol (MeOH: 0.05 to 1%), sodium chloride (NaCl: 0.5 to 2 g/L), liver digest (LD: 0.002% to 0.05%) and Dulbecco modified Eagle's minimal essential medium (DMEM: 0.002 to 0.05%).

3. Results and discussion

3.1 Data evaluation

The single particle calculation (SPC) spreadsheet has been thoroughly evaluated in several series of research and routine samples, in two international workshops, as well as in an interlaboratory method performance study [27]. Upon import of measurement data for calibration and unknown samples and entering information on material and instrument parameters the tool provides particle sizes, concentrations and particle size distribution, both numerically and graphically. In figure 1 the output of the tool is demonstrated in a screenshot of a typical application. The data tool allows the rapid evaluation of measurement data from individual samples which is a pre-requisite for the application of spICP-MS in routine analysis.

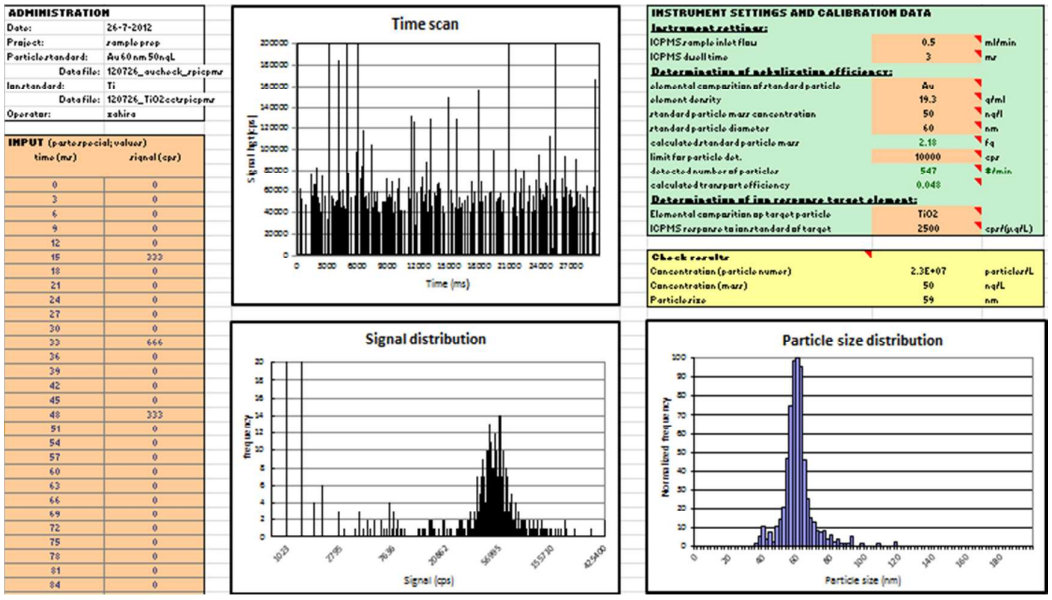

Figure 1: Screenshot of the calibration worksheet of the Single Particle Calculator spreadsheet showing the results for a 60 nm Au particle standard.

The SPC spreadsheet contains two worksheets, a calibration worksheet and a sample calculation worksheet. For each series of measurements one calibration worksheet is filled out and the parameters that are required are the nebulization

efficiency η_n and the response factor of an ionic analyte standard RF_{ION}. The nebulization efficiency is crucial for correct particle number determination and is determined by analyzing a diluted nanoparticle suspension. In principle any well characterized nanoparticle suspension can be used for this purpose and the data (chemical composition, particle size and mass concentration in the diluted standard suspension) have to be entered in the calibration worksheet. The suspension is then analyzed and the measurement data (Excel format or CSV) are imported in the calibration worksheet and $\eta_n$is calculated as:

$$\eta_n = \frac{N_p}{C_p} \times \frac{1000}{V}$$

Where η_n = nebulization efficiency; N_p = number of particles detected in the time scan (min^{-1}); C_p = particle number concentration (L^{-1}); V = sample input flow (mL/min). Alternatively, η_n can also be determined by a waste collection method which is also described in the standard operating procedure that can be downloaded with the SPC-spreadsheet. In practice, using a nanoparticle suspension (in this study RM8013) gave more accurate results. The other parameter needed in the calibration worksheet of the SPC-spreadsheet is the response factor of an ionic analyte standard, RF_{ION}, needed to calculate the mass of the individual particle's detected in a sample. Typically, a minimum of three different ionic concentrations are analysed to determine an average response factor and establish linearity of RF_{ION}. The average RF_{ION} is entered in the calibration sheet of the SPC-spreadsheet expressed in counts per second (CPS) per concentration unit (µg/L).

After importing the measurement data in the sample calculation worksheet a detection threshold value has to be entered to differentiate particles from the background. Specific cut-off criteria have been published and applied by other authors including criteria using 3 or 4 times the standard deviation of the recorded data, repeated outlier tests and transferring the data into a signal distribution graph[15,19]. In the latter method, the minimum in the signal distribution separates the background and ions (left side of the minimum) from the particles (right side of the minimum) and this method has been used in the SPC tool. The ICP-MS response separating particles from the background is found as the minimum in the signal distribution graph, the lower left graph in figure 1. This minimum is visually determined and entered in the sample calculation worksheet as the "limit for particle detection". The other required information is extracted from the calibration worksheet and the number of particles in the sample is calculated as:

$$C_p = \frac{N_p}{\eta_n} \times \frac{1000}{V}$$

Where C_p = particle number concentration (L^{-1}); N_p = number of particles detected in the time scan (min^{-1}); η_n = nebulization efficiency; V = sample input flow (mL/min). The mass of the individual particles in the sample is calculated as:

$$m_p = \frac{I_p\, t_d}{RF_{ion}} \times \frac{V\ \eta_n}{60} \times \frac{M_p}{M_a}$$

Where m_p = particle mass (ng); I_p = particle signal intensity in the sample (cps); RF_{ion} = ICP-MS response for ion standard (cps/µg/L); t_d = dwell time (s); V = sample flow (mL/min); η_n = nebulization efficiency; M_p = molar mass nanoparticle material; M_a = molar mass analyte measured. The particle size, expressed as the particle's diameter, and assuming a spherical particle shape, is calculated as follows:

$$d_p = \sqrt[3]{\frac{6\, m_p}{\pi\, \rho_p}} \times 10^4$$

Where: d_p = particle diameter in the sample (nm); m_p = particle mass (ng); ρ_p= particle density (g/mL). From the results for the individual particles, the mean particle diameter and the size distribution of the particles in the sample is calculated and graphically presented. To calculate the total particle mass concentration in the sample the masses of all individual particles are summed:

$$C_m = \frac{\sum m_p}{\eta_n \times V \times 1000}$$

Where C_m = particle mass concentration (ng/L); m_p = particle mass (ng); η_n = nebulization efficiency; V = sample flow (mL/min).

3.2 Method performance

The performance of the spICP-MS method on the quadrupole ICP-MS system was evaluated for four different types of particles, Au, Ag, TiO_2 and SiO_2 particles, according to the procedure described in the Experimental section. The investigated parameters include the limit of detection for particle size as well as for particle

concentration, the dynamic range, the precision and accuracy as well as the robustness. An overview of the results is given in table 1.

Table 1. Performance characteristics of spICP-MS method on a quadrupole and sector-field (LOD_{SIZE} only) ICP-MS instrument for four types of nanoparticles.

Particle type	Au	Ag	TiO_2	SiO_2
Linear size range tested	10-60 nm	20-110 nm	100-1000 nm	100-2500 nm
LOD_{SIZE} quadrupole instr.	20 nm	20 nm	50 nm	200 nm
LOD_{SIZE} sector-field instr.	10 nm	10 nm	20 nm	200 nm
LOD_{CONC}	1 ng/L (60 nm NP)	5 ng/L (60 nm NP)	50 ng/L (150 nm NP)	100 ng/L (500 nm NP)
Linear conc. range (cc >0.99)	10-1000 ng/L (60 nm NP)	5-500 ng/L (60 nm NP)	50-5000 ng/L (150 nm NP)	100-10000 ng/L (500 nm NP)
Precision mass conc. (n=6)	3% (60 nm NP at 50 ng/L)	5% (60 nm NP at 50 ng/L)	8% (100 nm NP at 500 ng/L)	5% (500 nm NP at 1000 ng/L)
Precision particle size (n=6)	3 % (60 nm NP)	2 % (60 nm NP)	2 % (150 nm NP)	1 % (500 nm NP)

Additional experiments were carried out with high-resolution sector field ICP-MS. These were carried out to see whether the same method and data processing also work for a different type of ICP-MS and whether smaller particles compared to measurement with a quadrupole ICP-MS. Results will be discussed in the following sections.

LOD_{SIZE}. The smallest nanoparticle that can be detected using spICP-MS is determined by the sensitivity of the ICP-MS system and the ability to differentiate particle signals from background noise. According to the equations in the previous section this can be found by plotting the particle signal intensity I_p as a function of the diameter to the 3th power (d^3). This method, that was proposed by Laborda et al., describes the minimum particle size is the point where the extrapolated particles signal intensity equals the background plus 3 times the standard deviation[19]. For Au NPs measured at a m/z 197, background noise is limited (and in case of the sector-field instrument virtually absent) allowing the detection of particles as small as 20 nm

with a standard quadrupole ICP-MS. For Ag (measured at m/z 107) the background noise in blanks is higher and analyses of a series of 20, 30, 60 and 110 nm Ag NPs indicates that 20 nm is the smallest Ag NP that can be detected. This result was confirmed by the interlaboratory exercise where most laboratories were able to correctly size a 40 nm Ag particle in water, but only a few were able to size a 20 nm Ag particle. Recently, Lee te al. described a method to estimate the LOD_{SIZE} and applied it to nanoparticles composed of 40 different elements[28]. Using a sector field ICP-MS even smaller nanoparticles can be measured and figure 2 shows the time scan and size distribution of a 10 nm gold particle (RM8011). That smaller sized particles can be measured with a sector-field instrument results from lower background signals and the instrument geometry. In a quadrupole the ion has to travel a complicated path to reach the detector while this path in a sector-field instrument is much more direct. As a result the ion transmission in a sector-field instrument is about 10 times higher than in a quadrupole instrument which translates into a factor of about 2 in size.

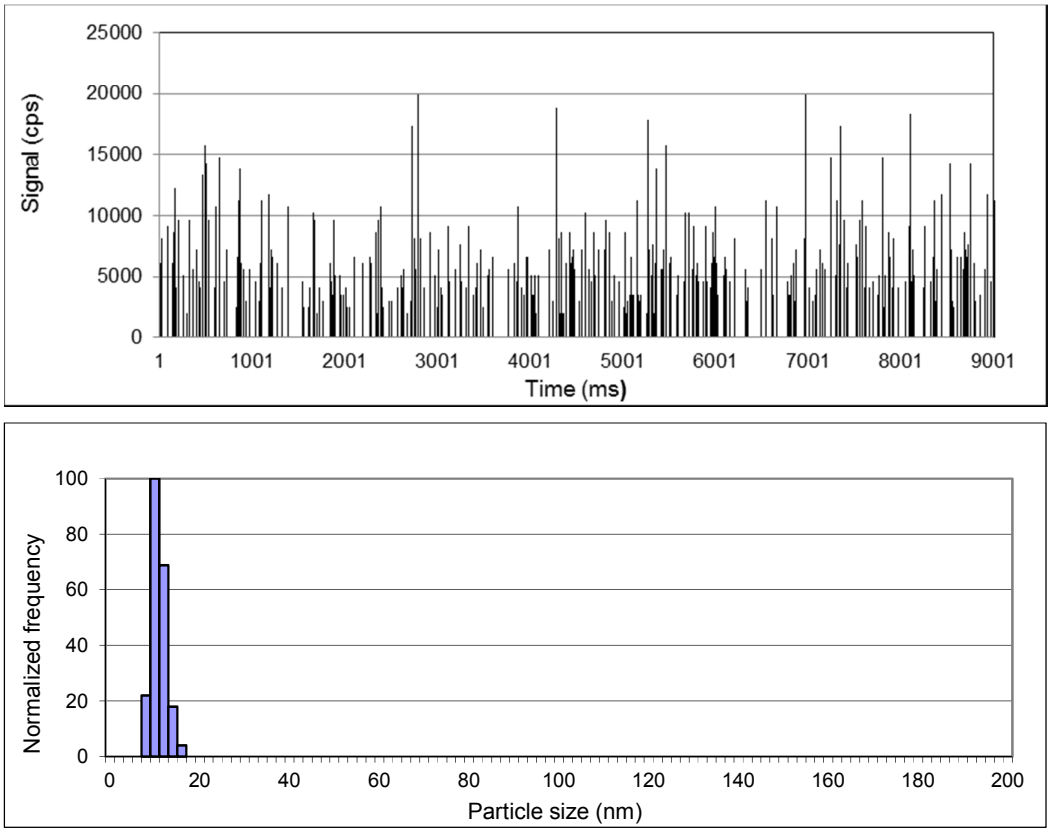

Figure 2. Time scan (top) and size distribution (bottom) of a 10 nm gold particle in MilliQ water at a mass concentration of 200 pg/L measured in single particle mode

using a sector-field instrument and a dwell time of 2 ms. Calculated modal particle size is 9.5 nm.

NM300, a reference material containing silver particles with a size around 16 nm is often used in exposure studies. However, a standard quadrupole instrument has a LOD_{SIZE} of 20 nm and will show only a small fraction of the Ag particles or aggregates with sizes >20 nm. The sector-field instrument was able detect and size the particles around 16 nm correctly. NM300 also contains a fraction of even smaller silver particles, size around 5 nm, which could not be detected even using the sector-field instrument. This is to be expected since a 5 nm silver particle contains only about 4000 atoms and taking into account the ionization and transmission efficiency in the sector-field instrument (about $5 \cdot 10^{-4}$) this means that only 1-2 ions will reach the detector, well in the range of instrument noise. In principle the ion transmission in a time-of-flight mass spectrometer is expected to be best, however, these are not very common and in a recent publication Borovinskaja et al. reported LOD_{SIZE} values for silver, gold and uranium that are larger than those for quadrupole ICP-MS systems[29].

For TiO_2 NPs which are measured at a relatively low mass (m/z 48), the background is higher and the LOD_{SIZE} is 50 nm for a quadrupole instrument. For silica measuring at m/z 28 the situation is even worse and the LOD_{SIZE} was found to be about 200 nm. The high background levels at m/z 28 arise from silica emissions from the quartz materials in the ICP-MS, as well as isobaric interferences from $^{14}N_2$ and $^{12}C^{16}O$ if samples with high carbon content are being processed. Replacing the nebulizer and the quartz spray chamber by quartz free materials and by using a reaction cell to remove bi-atomic ions does improve the background as does using a higher resolution with the sector-field instrument. In the latter case the isobaric interferences can be separated from the Si signals based on mass, however, an LOD_{SIZE} <100 nm could not be obtained. On the other hand, Aureli et al. showed that by replacing the quartz plasma torch tube by a ceramic type and by using a reaction cell with methane as the reaction gas, SiO_2 particles smaller than 100 nm can be measured[30].

LOD_{CONC}. Since the concentration is related to the number of signal pulses that are observed, this detection limit is related to the number of signal pulses in the blank and the total acquisition time. In the absence of nanoparticle contaminations and memory effects, the detection limit for a typical counting process as spICP-MS is 3 pulses during the total acquisition time[31]. Based on the experimental settings and a nebulization efficiency of 2%, LOD_{CONC} is 100 particles/mL corresponding to a mass

concentration of about 0.2 ng/L for 60 nm Au NPs. However, in practice this is not realistic since blanks will be affected by memory effects and the wash-out time of NPs adsorbed in the ICP-MS sampling system. Using a good quality MilliQ water we observed 5 ± 5 particles/min in blank samples positioned in between 60 nm Au NPs standards resulting in an actual LOD_{CONC} of 1 ng/L. For SiO_2 and TiO_2 NPs the number of signal pulses observed in blank samples was comparable, 10 ± 3 and 4 ± 4 respectively. For Ag NPs the number of signal pulses in blank samples was substantially higher, 26 ± 23, especially in blanks positioned in between Ag NP standards indicating adsorption effects in the sampling system of the ICP-MS. The LOD_{CONC} values for the different NPs are given in table 1. Please note that the LOD_{CONC} values for TiO_2 and SiO_2 expressed as a mass concentration are 1 to 2 orders of magnitude higher than those for Au and Ag which is a consequence of the larger particle sizes. If the LOD_{CONC} values are expressed as a particle concentration, the LOD_{CONC} values for all NPs are comparable.

Concentration dynamic range. The concentration dynamic range is limited by the single particle definition, i.e. the need to avoid multiple particles in each event. Since particles arrive independently of one another, Poisson statistics can be used to estimate the probability of one or multiple nanoparticles arriving to the plasma during one dwell time period and being detected as one particle. Laborda et al. calculated probabilities for such events to occur and discussed the selection of a critical nanoparticle number concentration to minimize the occurrence of multiple nanoparticle events[32]. In practice, if the number of multiple nanoparticle events becomes significant, deviation from linearity will be observed as the particle concentration increases. Linear concentration ranges were determined for all four types of NPs using this setting. The calibration curve of 60 nm Au NPs was linear from 10 up to 1000 ng/L which resulted in ~95 signal pulses s^{-1}. The calibration curve for 60 nm silver particles is very similar, showing linearity up to ~100 signal pulses s^{-1} and for silver NPs the calibration curve was linear from 5 to 500 ng/L (as expected since the density of Au is twice that of Ag, resulting in identical particle numbers). For the TiO_2 and SiO_2 calibration curves particle with sizes of ~140 and 500 nm were used and linear concentration ranges were 0.05 to 5 µg/L for TiO_2 and 0.1 to 10 µg/L for SiO_2 (see table 1).

Size dynamic range. Apart from the maximum number of particles, it is also important to know what the maximum particle size can be since the vaporization of large particles during flight in the plasma may be partial only. For Au, Ag and TiO_2

NPs, the response factors for the different sized particles were all equal, indicating that they were all completely vaporized. This however, was not the case for silica. While particles in the range of 500-2000 nm gave the same response factor, a 5000 nm particle gave a lower response factor. Based on the signal intensity a particle size of ~2500 nm is found for the 5000 nm particle. Degueldre et al. have evaluated this problem by calculating the vaporization time for UO_2 particles as a function of particle size[33]. Assuming a residence time of the particle in the plasma of 10^{-4} s their calculations indicate that the upper particle size would be ~2000 nm. Aeschliman et al. used high-speed digital photography to study the vaporization of micrometer sized Y_2O_3 particles and reported that these were completely vaporized[34]. Carcia et al. studied ICP particle vaporization of SiO_2 particles by measuring the intensities of silicon emission lines with different excitation energies. Their measurements indicated that SiO_2 particles up to 2000 nm will be vaporized completely in the ICP plasma[35]. Therefore it seems safe to adopt a maximum particle size for SiO_2 of 1000 nm, although it should be kept in mind that micro sized particles may produce a signal intensity outside the linear range of the detector.

Precision. The precision was determined by replicate analysis (n=6) of standards in MilliQ water with an acquisition time of 60 s and is presented in table 1. For 60 nm Au NPs at a mass concentration of 50 ng/L the precision expressed as the relative standard deviation was found to be 3%. For the 60 nm Ag, 100 nm TiO2 and 500 nm SiO2 NPs, the precision of the concentration was 5%, 8% and 5%, respectively. The precision for the size determination, i.e. the height of the signal pulses is also determined as the standard deviation in replicate analysis (n=6) of standards in MilliQ water and ranged from 1% for the larger SiO_2 particles to 3% for the 60 nm Au NPs (see table 1).

Accuracy. In spICP-MS, particle size determination relies on a number of assumptions. The primary measured particle property is the signal intensity from which the particle mass is calculated using standard curves prepared from ion standards. Based on assumptions on stoichiometry, density and shape the particle size is calculated. Therefore, accuracy can only be determined using particles with a certified, or well defined particle size. There are only a very limited number of such particles available and in this study NIST reference materials RM8011, -8012 and -8013 with nominal diameters of 10, 30 and 60 nm are used. For the 10 nm Au NP an accurate size of 9.5 ± 1.0 nm was determined using a sector-field ICP-MS instrument and calibration based on ion standards. In the same way the accurate sizes of the 30

and 60 nm Au NP were determined as 28.2 ± 1.4 and 56.1 ± 2.8 nm using a quadrupole ICP-MS system and calibration based on ion standards. However, calculating accuracy is not possible since the reference values given by NIST depend on the measurement method. For the 10 nm Au NP these values range from 8.5 – 13.5 nm, for the 30 nm Au NP from 24.9 – 28.6, and for the 60 nm Au NP from 53.2 – 56.6 nm. The sizes as determined with spICP-MS fit within these ranges. However, without any a priori knowledge about particle composition and shape no conclusions can be drawn about the true particle size. It is for this reason that spICP-MS, despite its being easy and fast, remains a screening method. This can be improved by combining spICP-MS with size separation techniques like HDC or AF4 which allows the determination of true particle sizes[36]. This however, may be limited by the dynamic range, and will require further development of data processing software.

Robustness. Although samples often have to be diluted to a large extent to fit into the dynamic range of spICP-MS, the sample matrix may still interfere with the nebulization because of differences in droplet surface tension and particle surface properties. Particles may have become coated with matrix constituents, for instance proteins in a biological matrix. If a matrix component changes the nebulization efficiency from 2.5% to 2.0%, then a relative decrease in the particle count rate of ~20% is expected, i.e. an underestimation of the particle concentration. Matrix components may also interfere with the ionization in the ICP-MS plasma which often leads to suppression and sometimes enhancement of the analyte signal, resulting in an underestimation or overestimation of particle size, respectively. Both effects were studied by the determination of the particle concentration and particle size of 60 nm Au, 60 nm Ag and <100 nm TiO_2 NPs at three concentration levels in water containing the matrix components sodium dodecyl sulphate (SDS: 1 to 10 mM), methanol (MeOH: 0.05 to 1%), sodium chloride (NaCl: 0.5 to 2 g/L), liver digest (LD: 0.002% to 0.05%) and Dulbecco modified Eagle's minimal essential medium (DMEM: 0.002 to 0.05%). The results for the Au NPs are summarized in figure 3 and expressed relative to what is found in pure water. As expected MeOH results in an increase of the observed particle concentration since it lowers the sample viscosity, thereby increasing the nebulization efficiency. In addition, an increase in the particle size is observed at the highest MeOH concentration which may result from a carbon-enhancement ionization effect on hard to ionize elements like Au[37]. SDS and DMEM show a similar effect, however since the highest effects were observed at the lowest particle concentrations, this effect probably originates from particle stabilization in the

sample suspensions and decreasing adsorption in the ICP-MS sampling system. This is expected since SDS is a surfactant and DMEM contains proteins and other materials with surfactant-like properties. The presence of a liver extract and NaCl does not seem to have any influence on the particle count during spICP-MS measurement. On the other hand, NaCl is the only matrix component that is of influence on the observed particle size. This originates from ionization suppression in the plasma leading to lower signal intensities and thus smaller particle sizes.

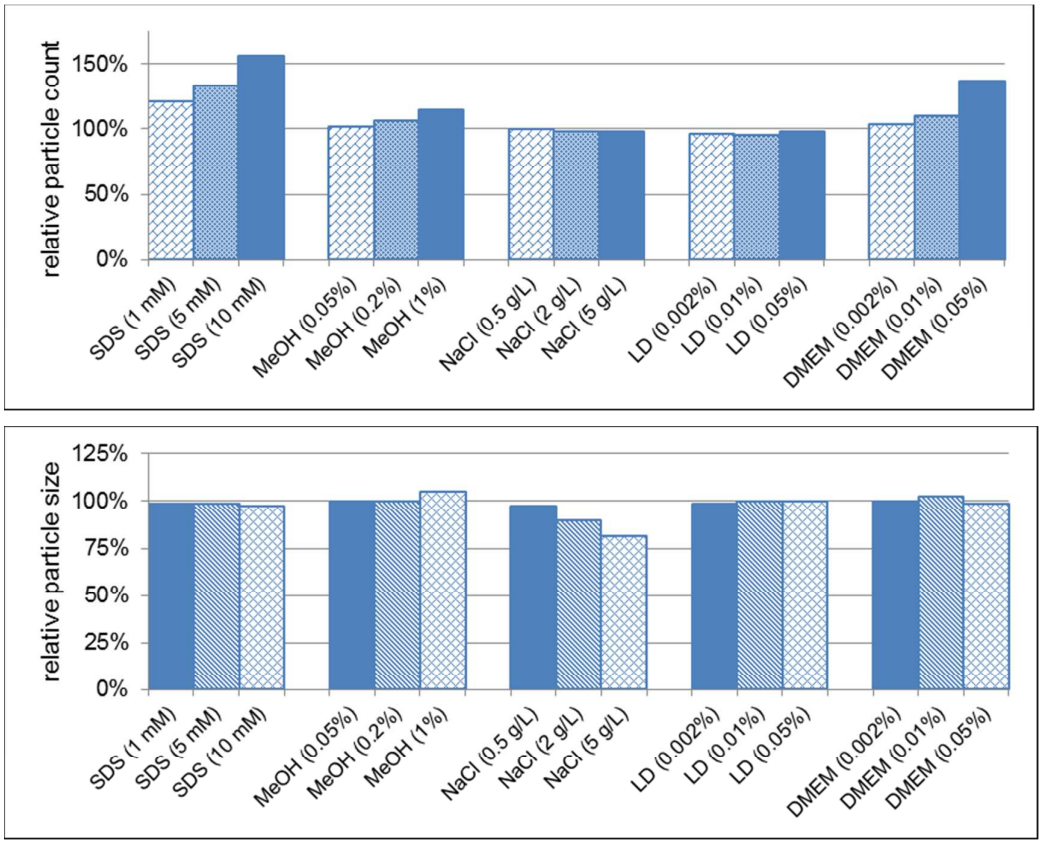

Figure 3. Matrix effects in spICP-MS analysis on the observed particle count (top) and particle size (bottom) of a 60 nm Au NP.

3.3 Applications of spICP-MS in complex samples

Food. Chicken meat samples spiked with silver NP were prepared as reference materials in the frame of the NanoLyse project to mimic migration to food from food contact materials, e.g. cutting boards or food packaging containing Ag NP for antimicrobial activity. Within this study these materials were analyzed by spICP-MS

for Ag NP concentrations and stability. After enzymatic digestion and dilution, the samples were easily amenable to the developed spICP-MS methods. In freshly spiked blank samples the size distribution was similar to that in the spiking dispersion and the concentration in agreement with the spiked amount (figure 4). Samples that had been stored for an extended period showed a decrease in Ag NP concentration and a shift of the size distribution to smaller diameters suggesting dissolution and possible agglomeration of Ag NPs[22]. No matrix effect from the chicken samples was observed.

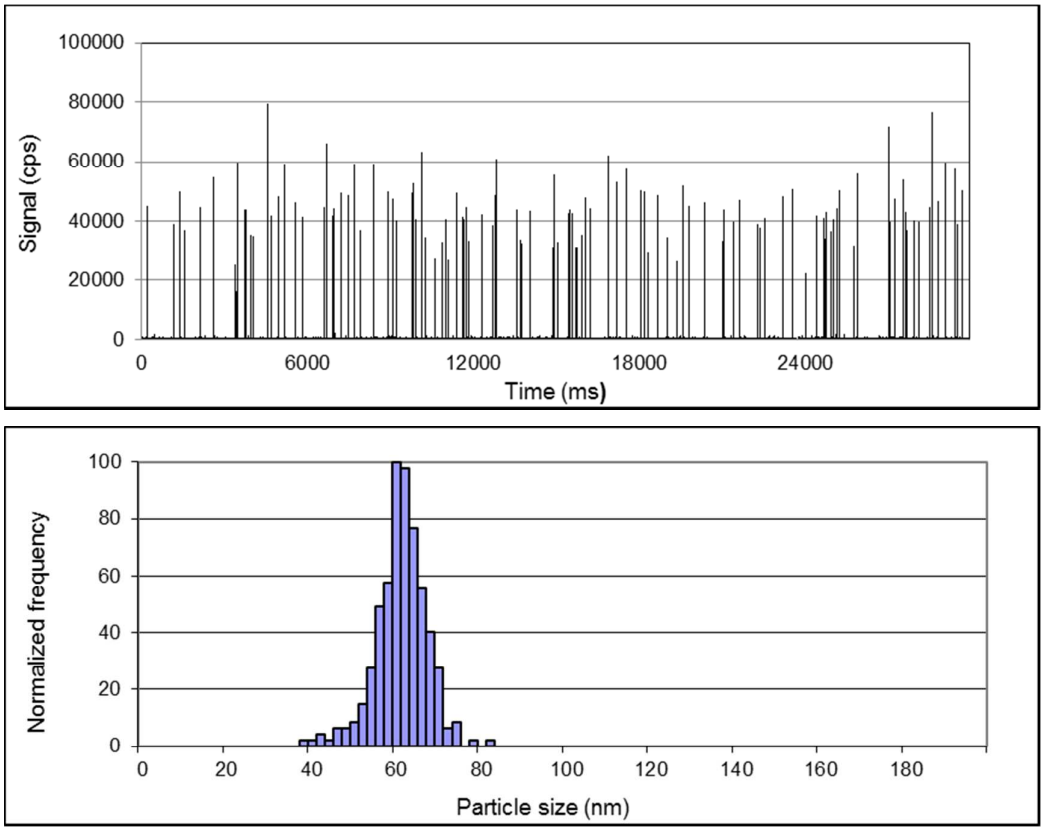

Figure 4. Time scan (top) of the spICP-MS analyses of a diluted digest of chicken meat containing 60 nm silver NP at a mass concentration of 10 mg/kg and the particle size distribution (bottom) calculated from the time scan showing a modal size of 62 nm for the silver NP.

Waste water. From a risk assessment point of view, solubility is a property of importance. If a nanomaterial is soluble then there is no need to consider it as nano and thus can be treated in the same way as chemicals. However, discriminating between particulate material and free (hydrated) ions or soluble complexes in a

sample is not straightforward. Often separation techniques as membrane filtration or ultracentrifugation are needed to separate the particulate and dissolved fractions. spICP-MS can be used to differentiate between nanoparticles and free ions of the same element in one sample[19]. This is based on the constant signal produced by the dissolved analyte which induces a shift of the continuous background in the time scan to a higher value while maintaining the pulses due to the particles. By plotting the number of readings for each intensity as done in the frequency distribution in the Single Particle Calculation spreadsheet, two distributions are obtained (see figure 5, middle). The first one, at lower intensities, is due to the dissolved analyte, whereas the second one is due to the nanoparticles. The concentration of the dissolved analyte can be calculated directly using the ICP-MS response of the dissolved standard in the calibration worksheet of the calculation spreadsheet. Figure 5 shows the time scan, signal frequency distribution and size distribution of silver nanoparticles in waste water in the presence of dissolved silver. The total silver concentration in the original sample was 500 µg/L. From the spICP-MS data it followed that about 50 µg/L was particulate material with particle sizes around 40 nm while the other 450 µg/L was ionic silver. It should be noted that the increase of the background (and especially the increase of the variance of the background) by dissolved species will negatively affect the smallest particle size that can be detected. In addition, very small particles that are below the LOD_{SIZE} of the spICP-MS method will be undetected and form part of the "dissolved" fraction. Finally, there is a difference between detection limit of nanoparticles and the corresponding dissolved analyte. While the LOD_{CONC} for nanoparticles is in the low ng/L range, the limit of detection for dissolved analytes will generally be in the high ng/L range. As a result, low dissolved analyte concentrations can generally not be measured because of the dilution factor required to observe the particles.

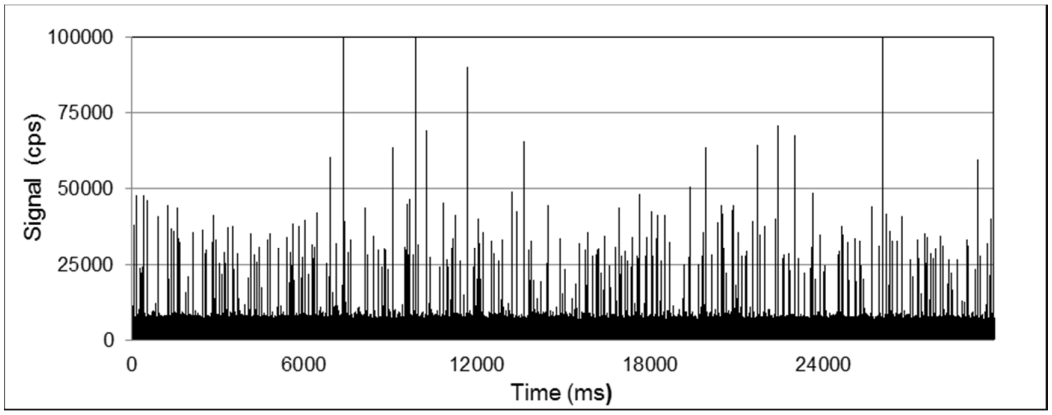

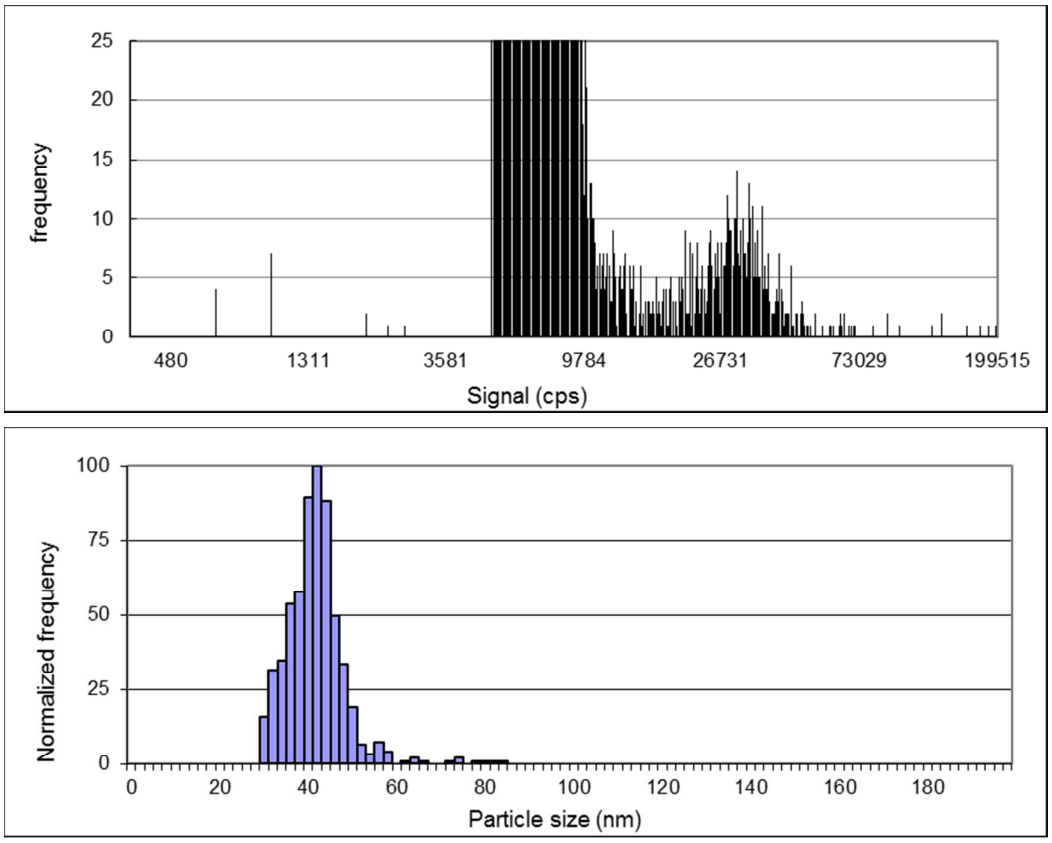

Figure 5. Time scan (top), signal frequency distribution (middle) and particle size distribution (bottom) of Ag NP in a sample of waste water after dilution.

Culture media. Another interesting area for spICP-MS is the detection of nanoparticles in biological test systems, for instance *in-vitro* (nano) toxicology. Due to the high degree of dilution during sample preparation the influence of salts, organic compounds and biological matrices like DMEM present in cell culture medium are minimized. To illustrate the potential of spICP-MS in these kinds of studies, we show some results from an *in vitro* experiment studying the translocation of TiO_2 across a monolayer of Caco-2 cells. Brun et al studied this translocation using transmission electron microscopy and synchroton-based micro X-ray fluorescence[38]. Figure 6 show time scans of samples collected from the apical and basolateral pole of these cells collected 24 hours after addition of the NPs. Sample preparation consisted of collection of a subsample, sonication and dilution. Figure 6 (top) shows the presence of a high particle concentration of TiO_2 NPs in the sample from the apical pole while figure 6 (bottom) shows only a few signal pulses in the sample collected from the basolateral pole, indicating that translocation of the TiO_2 NPs appears to be minimal. In fact, the number of signal pulses was not significantly different from blank control samples in the experiment and in that case the translocation was quantified by

considering the number of signal pulses plus three times the standard deviation in the number of signal pulses in blank samples as the detection limit, LOD_{CONC}. In this experiment LOD_{CONC} was 15 signal pulses while the number of signal pulses in the apical sample during the acquisition time was ~1000 indicating that translocation, if any, is smaller than 2%.

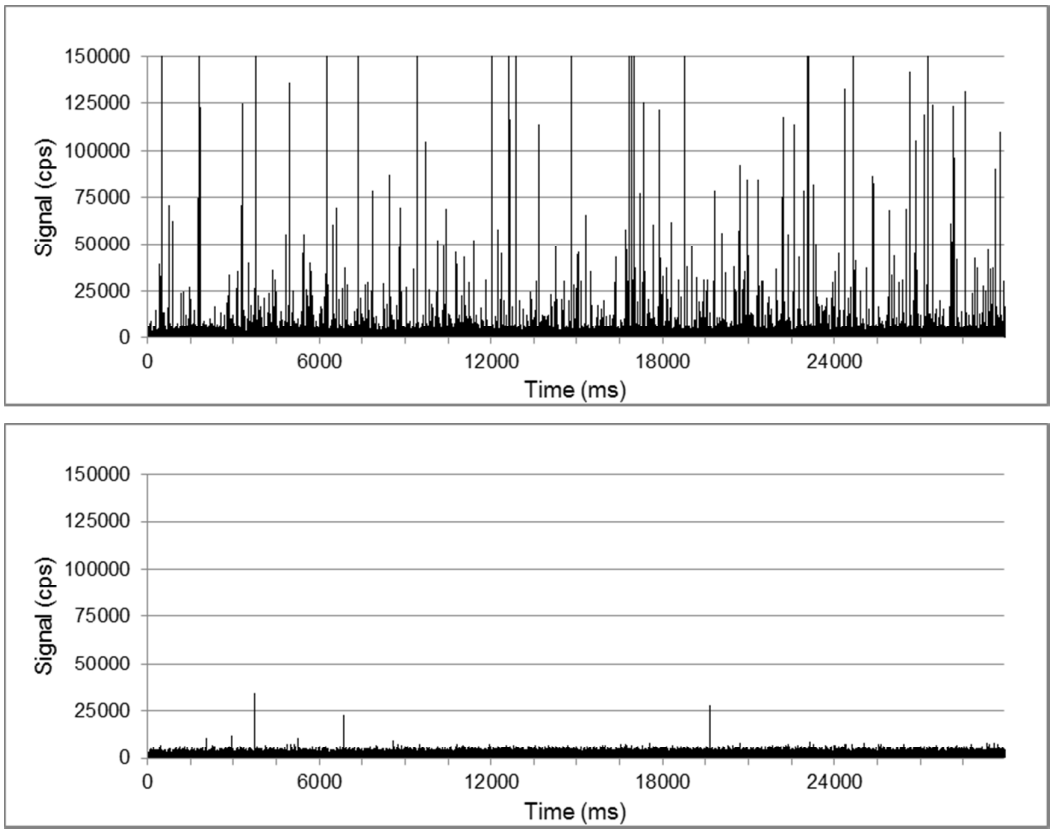

Figure 6. spICP-MS time scan of the apical (top) and basolateral (bottom) phases of an in vitro *translocation test with TiO_2 NPs.*

Biological tissues. At present, little is known about the kinetics and bioavailability of nanoparticles after oral exposure. The difficulty here is that many toxicological studies with NPs are severely hindered by the poor availability of analytical methods that can quantify NPs in tissues[39]. To show the applicability of spICP-MS analysis for the detection of NPs in tissues we analyzed liver samples of rats exposed to Ag NPs[40]. A subsample was collected from the liver samples, enzymatically digested, and the digest diluted and measured using spICP-MS. The raw data, in the form of the time scan in figure 7, immediately indicates the presence of nanoparticles containing silver and further calculation showed that these had a modal size of 38 nm with a few particles having sizes over 100 nm. These are likely aggregates because

the NM300 materials the rats were exposed to have a particle size around 16 nm. Interestingly, low concentrations of these particles were also found in the liver of animals that were exposed to $AgNO_3$, while no particles were found in the liver of non-exposed animals. Although further research is required to elucidate the kinetics of NPs after oral exposure, spICP-MS proved to be a sensitive tool for detection and characterization of NPs after oral exposure in biological tissues.

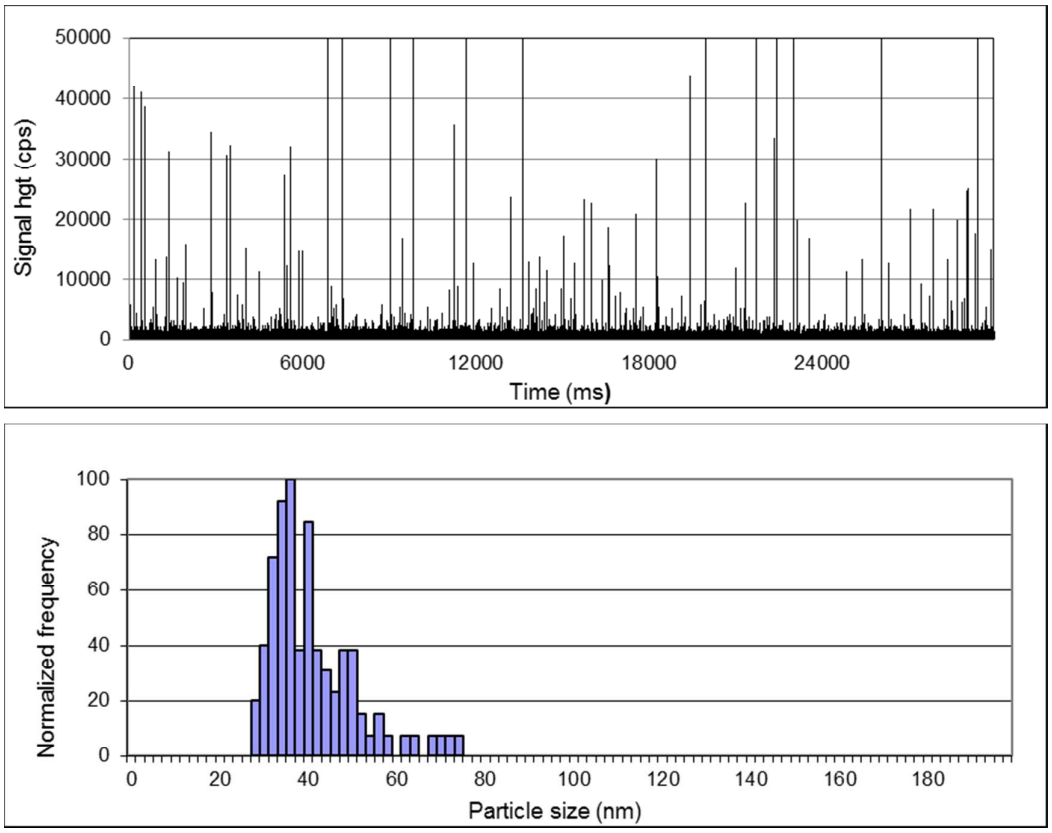

Figure 7. Time scan (top) of the enzymatic digest of a rat liver sample after oral administration of Ag NPs through the food and drinking water. The size distribution (bottom), which is skewed to larger particle sizes, indicates a modal particle size of 36 nm.

4. Concluding remarks

spICP-MS was studied as a screening tool for the detection and characterization of nanoparticles and a data evaluation tool was developed. spICP-MS combined with the Single Particle Calculation tool for data processing is an easy and fast screening technique capable of detecting and characterizing metal and metal oxide NPs at low

concentrations in complex samples. The performance characteristics were determined for four types of NPs and with two different types of ICP-MS systems. The size detection limits were 20 nm (Au and Ag), 50 nm (TiO_2) and 200 nm (SiO_2) for a quadrupole instrument. A sector-field instrument performed better with size detection limits of 10 nm (Au and Ag), 20 nm (TiO_2) and 200 nm (SiO_2). The main reason for this increased performance is the geometry of the sector-field instrument which allows higher ion transmission. Concentrations detection limits ranged from 1 ng/L for 60 nm Au NPs to 0.1 µg/L for 500 nm SiO_2 particles and the dynamic range of spICP-MS is two orders of magnitude, limited by the "single particle" principle. The precision for particle size is <5% while the precision for particle concentration is <10%. The influence of matrix compounds on the accuracy of particle count and size was limited, only soap-like compounds as SDS showed a substantial influence on the particle count. Finally, four applications showed that spICP-MS is an easy and fast screening technique capable of detecting and characterizing metal and metal oxide NPs in complex samples, generally without extensive sample preparation.

Acknowledgements

This research was commissioned and financed by the Netherlands Ministry of Economic Affairs and the Netherlands Food and Consumer Product Safety Authority.

References

1. H. D. Chen, J. C. Weiss and F. Shahidi. *Food Technol.,* 2006, 60, 30-36.
2. SCENHIR. Opinion on the scientific aspects of the existing and proposed definitions relating to products of nanoscience and nanotechnologies, 2007, November 29. http://ec.europa.eu/health/ph_risk/committees/04_scenihr/docs/scenihr_o_012.pdf
3. EFSA. Scientific opinion on the potential risks arising from nanoscience and nanotechnologies on food and feed safety, 2009, February 10. http://www.efsa.europa.eu/de/scdocs/doc/958.pdf.
4. E. K. Richman and J. E. Hutchison. *ACS Nano*, 2009, 3, 2441-2446.
5. European Commission. *Official J European Union*., 2011, L275, 38-40.
6. M. Hassellöv, J. W. Readman, J. Ranville and K. Tiede. *Ecotoxicology,* 2008, 17, 344-361.

7. F. Von der Kammer, S. Legros, T. Hofmann, E. H. Larsen and K. Loeschner. *Trends Anal Chem.,* 2011, 30, 425-450.
8. F. Von der Kammer, L. Ferguson, P.A. Holden, A. Masion, K. R. Rogers, S. J. Klaine, A. Koelmans, N. Horne and J. M. Unrine. *Environ. Toxicol. Chem.,* 2012, 31, 32-49.
9. S. Dekkers, P. Krystek, R. J. B. Peters, D. P. K. Lankveld, B. G. H. Bokkers, P. H. Van Hoeven-Arentzen, H. Bouwmeester and A. G. Oomen. *Nanotoxicology,* 2011, 5, 393-405.
10. K. Loeschner, J. Navratilova, C. Købler, K. Mølhave, S. Wagner, F. von der Kammer and E. H. Larsen. *Anal. Bioanal. Chem.,* 2013, 405, 8185-8195.
11. C. Contado, L. Ravani and M. Passarella. *Anal. Chim. Acta.,* 2013, 788, 183–192
12. V. Filipe, A. Hawe and W. Jiskoot. *Pharmaceutical Research,* 2010, 27, 796–810.
13. R. C. Flagen. *KONA Powder and Particle Journal,* 2008, 26, 254-268.
14. J. McCarthy and C. Degueldre. *Characterisation of Environmental Particles, Vol 2*. Lewis Publishers, Chelsea MI, 1993, Chapter 6, pp 247-315.
15. H. E. Pace, N. J. Rogers, C. Jarolimek, V. A. Coleman, C. P. Higgins and J. F. Ranville. *Anal. Chem.,* 2011, 83, 9361-9369.
16. A. Scheffer, C. Engelhard, M. Sperling and W. Busher. *Anal. Bioanal. Chem*., 2008, 390, 249-252.
17. L. Yu and A. Andriola. *Talanta*, 2010, 82, 869-875.
18. Y. Suzuki, H. Sato, S. Hikida, K. Nishiguchi and N. Furuta. *J. Anal. At. Spectrom*., 2010, 25, 947-949.
19. F. Laborda, J. Jiménez-Lamana, E. Bolea and J. R. Castillo. *J. Anal. At. Spectrom*., 2011, 26, 1362-1371.
20. D. M. Mitrano, E. K. Lesher, A. Bednar, J. Monserud, C.P. Higgins and J. F. Ranville. *Environ. Toxicol. Chem.,* 2011, DOI : 10.1002/etc.719.
21. E. P. Gray, J. G. Coleman, A. J. Bednar, A. J. Kennedy, J. F. Ranville and C.P. Higgins. *Environ Sci Technol*., 2011, DOI:10.1021/es403558c
22. R. J. B. Peters, Z. Herrera-Rivera, G. van Bemmel, H. J. P. Marvin, S. Weigel and H. Bouwmeester. *Anal. Bioanal. Chem.,* 2014, DOI 10.1007/s00216-013-7571-0.
23. T. P. J. Linsinger, R. Peters and S. Weigel. Anal. Bioanal. Chem., 2014, 406, 3835-3843.
24. R. J. B. Peters, Z. Herrera-Rivera, H. Bouwmeester, S. Weigel and H. J. P. Marvin. *Qual. Ass. Safe. Crop. Food.,* 2014, 6, 281-290.

25. F. Laborda, E. Bolea, J. Jiménez-Lamana. Anal. Chem., 2014, 86, 2270-2278.
26. R. Grombe, G. Allmaier, J. Charoud-Got, A. Dudkiewicz, H. Emteborg, T. Hofmann, E. H. Larsen, A. Lehner, M. Llinàs, K. Mølhave, R. J. Peters, J. Seghers, C. Solans, F. von der Kammer, S. Wagner, S. Weigel, T. P. J. Linsinger. *Anal. Chim. Acta.,* 2014, submitted.
27. T. P. J. Linsinger, R. J. Peters and S. Weigel. *Anal. Bioanal. Chem.,* 2014, 406, 3835-3843.
28. S. Lee, X. Bi, R.B. Reed, J.F. Ranville, P. Herckes and P. Westerhoff. Environ. Sci. Technol., 2014, 48, 10291-10300.
29. O. Borovinskaya, S. Gschwind, B. Hattendorf, M. Tanner and D. Günther. *Anal. Chem.,* 2014, 86, 8142–8148.
30. F. Aureli, M. D'Amato, B. De Berardis, A. Raggi, A. C. Turco, F.J. Cubadda. *Anal. At. Spectrom*., 2012, 27, 1540-1548.
31. L. A. Currie. *Anal. Chem*., 1968, 40 (3), pp 586–593
32. F. Laborda, J. Jiménez-Lamana, E. Bolea and J.R. Castillo. J*. Anal. At. Spectrom*., 2013, 28, 1220-1232.
33. C. Degueldre, P. Y. Favalger, R. Rossé and S. Wold. *Talanta,* 2006, 68, 623-628.
34. D. B. Aeschliman, S. J. Bajic, D. P. Baldwin and R. S. Houk. *J. Anal. At. Spectrom*., 2003, 18, 1008-1014.
35. C. C. Garcia, A. Murtazin, S. Groh, V. Horvatic and K. Niemax. *J. Anal. Atom. Spectrom*., 2010, 25, 645-653.
36. D. Rakcheev, A. Philippe and G. E. Schaumann. *Anal. Chem*., 2013, 85, 10643-10647.
37. E.H. Larsen and S. Stürup. J. Anal. At. Spectrom., 1994, 9, 1099-1105.
38. E. Brun, M. L. Jugan, N. Herlin-Boime, D. Jaillard, B. Fayard, A. M. Flank, A. Mabondzo and M. Carrière. *J. Physics: Conf. Series*, 2011, 304, 1-7.
39. H. Bouwmeester, S. Dekkers, M. Y. Noordam, W. I. Hagens, A. S. Bulder, C. de Heer, S. E. C. G. ten Voorde, S. W. P. Wijnhoven, H. J. P. Marvin and A. J. A. M. Sips. *Regulatory Toxicology and Pharmacology*, 2009, 53, 52-62.
40. M. Van der Zande, R. J. B. Peters, A. A. Peijnenburg and H. Bouwmeester. *Toxicology Letters*, 2011, 205, S289.

Single particle ICP-MS as a routine tool for the analysis of nanoparticles in complex matrices

Ruud Peters, Zahira Herrera-Rivera, Anna Undas, Martijn van der Lee, Hans Marvin, Hans Bouwmeester, Stefan Weigel

RIKILT – Institute of Food Safety, Wageningen UR, PO Box 230, 6700 AE Wageningen, the Netherlands

Graphical and textual abstract for the Table of contents entry

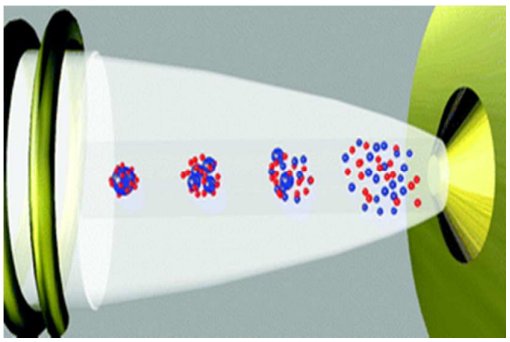

spICP-MS measurement with a powerful data evaluation tool is presented as a fast, cost efficient and easy to use screening tool for metal and metal oxide NPs in complex matrices.